

1 Article

## 2 Investigating the role of shape and size of gold 3 nanoparticles on their toxicities to fungi

4 Kangze Liu <sup>1,\*</sup>, Zhonglei He <sup>1</sup>, Hugh J. Byrne <sup>2</sup>, James Curtin <sup>1</sup> and Furong Tian <sup>1,\*</sup>

5 <sup>1</sup> Environmental Sustainability and Health Institute, School of Food Science and Environmental Health,  
6 College of Sciences and Health, Dublin Institute of Technology, Cathal Brugha Street, Dublin 1, Ireland;

7 <sup>2</sup> FOCAS Research Institute, Dublin Institute of Technology, Camden Row, Dublin 8, Ireland;

8 \* Correspondence: kangze.liu@dit.ie; furong.tian@dit.ie; Tel.: [+353 \(01\) 4027543](tel:+353014027543)

9 **Abstract:** The possibility of releasing gold nanoparticles (GNP) into the environment has been  
10 rapidly increasing with the wide spread and flourishing application of gold nanoparticles (GNPs)  
11 in a wide range of areas. Consequently, environmental effects of GNP, especially toxicities to  
12 living organisms have drawn great attention. However, their toxicological characteristics still  
13 remain unclear. Fungi, as the decomposers of the ecosystem, interact directly with the  
14 environment and critically control the overall health of the biosphere. Thus, their sensitivity to  
15 GNP toxicity is particularly important. The aim of this study was to evaluate the role of shape and  
16 size of GNPs on their toxicities to fungi, which could help reveal the ecotoxicity of GNPs.  
17 *Aspergillus niger*, *Mucor hiemalis* and *Penicillium chrysogenum* were chosen for toxicity assessment,  
18 and circular and star/flower-shaped GNPs sized from 0.7 nm to large aggregates of 400 nm have  
19 been synthesised. After mixed with GNPs and reacting agents of GNPs accordingly and incubated  
20 for 48 hours, the relative survival rates of each kind of fungus was calculated and compared. The  
21 results indicated that with similar sizes, star/flower-shaped GNPs are more toxic to fungi than  
22 circular-shaped GNPs; the toxicity of star/flower-shaped GNPs increases with smaller sizes. The  
23 results also showed that different species of fungus reacts differently to same GNPs, and  
24 *Penicillium chrysogenum* was relatively more sensitive under the exposure to GNPs.

25 **Keywords:** gold nanoparticle; fungi; nanoparticle shape; nanoparticle size; nanotoxicology

26

---

### 27 1. Introduction

28 In the flourishing field of nanotechnology, gold nanoparticles (GNPs) have received a lot of  
29 attention, particularly due to potential applications in bio-related areas [1-5]. The unique physical  
30 and chemical properties of noble metal nanoparticles such as GNPs, with specific electronic  
31 structures different from atoms or bulk states, have long been of interest and have been widely  
32 exploited in diversiform areas such as electronics, chemistry, optics, biomedicine [1-5]. One of the  
33 most important characteristics of GNP is the localised surface plasmon resonance (LSPR). LSPR  
34 phenomena of GNPs are manifest when the dimensions of the GNP are smaller than the extent of  
35 the plasmon wavefunction delocalisation, resulting in strong resonances of the surface electronic  
36 states with radiation in the visible region of the spectrum. [6,7]. Although silver nanoparticles show  
37 stronger LSPR phenomena, with a stronger absorption, GNPs are more commonly used in  
38 biological related applications because of their reputed biocompatibility [6-8].

39 Nevertheless, while silver nanoparticles have been widely used as anti-microbial materials due  
40 to their high toxicity [9-11], the toxicity of GNPs has not yet been fully understood and has drawn  
41 the attention of researchers. Notably, it has been reported that the toxicity of GNPs on microbes  
42 depends strongly on the species of microbe and the physicochemical properties of the GNP [12-14],  
43 and it has also been reported that different shapes of GNPs, such as spheres, rods, triangles,  
44 hexagons, prisms, and so on, have different cellular uptake mechanisms and elicit different toxic  
45 responses [15-18].

46 With the rapidly increasing applications of GNPs, the possibility of their release into the  
47 environment has grown dramatically [19-21]. Thus, their effects on the environment, especially  
48 their ecotoxicity, have drawn increasing attention [22-24]. Therefore, the toxicity of GNPs to  
49 organisms that strongly interact with their direct environment, such as fungi and plants, is of  
50 critical importance [23,24].

51 Fungi are found in most terrestrial, marine and freshwater environments and are the dominant  
52 decomposers within the ecosystem. They play a key role in energy cycling and ensuring that  
53 nutrients are released from dead and dying plants and animals, thereby ensuring these nutrients  
54 remain in circulation within the biosphere [25]. Bioaccumulation of contaminating heavy metals has  
55 been observed in terrestrial and water-borne fungi due in part to the large surface area of fungal  
56 mycelia, their role as decomposers of dead organic matter and their ecological niche to extract,  
57 concentrate and recycle nutrients and minerals back into the biosphere [26]. Organisms within an  
58 ecosystem that accumulate toxicants are typically more likely to suffer adverse effects at lower  
59 environmental concentrations, thus, the sensitivity of common fungi to GNP exposure is critical, as  
60 it may impact negatively on the biosphere's capacity to recycle organic and inorganic materials. In  
61 this study, 3 kinds of fungi, namely *Aspergillus niger*, *Mucor hiemalis* and *Penicillium chrysogenum*, are  
62 chosen for toxicity assessment, since they are common fungi species, wide-spread in the  
63 environment [27-29]. Comparing to the standard synthesis method of HEPES reduced GNPs, which  
64 only use HEPES and chloroauric acid [30,31], circular-shaped GNPs with different sizes are also  
65 synthesised by adding different concentrations of monosodium phosphates. Similarly, star/flower-  
66 shaped GNPs of various sizes are synthesised by adding different concentrations of disodium  
67 phosphates. The toxicities of these GNPs on the 3 chosen fungi species are examined and compared  
68 to determine the role of size and shape on GNP toxicity.

## 69 2. Materials and Methods

### 70 2.1. Materials

71 Hydrogen tetrachloroaurate(III) trihydrate ( $\text{HAuCl}_4 \cdot 3\text{H}_2\text{O}$ ) was purchased from Fisher  
72 Chemical, Ireland. N-2-hydroxyethylpiperazine-N-2-ethanesulphonic acid (HEPES) buffer was  
73 purchased from Hampton Research, US. Sodium hydroxide (NaOH), hydrochloric acid (HCl),  
74 sodium phosphate monobasic ( $\text{NaH}_2\text{PO}_4$ ) and disodium hydrogen phosphate ( $\text{Na}_2\text{HPO}_4$ ) were  
75 purchased from Sigma Aldrich, Ireland. *Aspergillus niger* ATCC 16404, *Mucor hiemalis* LZB 130,  
76 *Penicillium chrysogenum* LZB 141 strains were purchased from Blades Biological Ltd., UK. Potato  
77 dextrose agar (PDA) was purchased from Lab M, UK.

78 Sterilised deionised water, deionised using Elix® Reference Water Purification System from  
79 Millipore, Ireland, and sterilised using Autoclave SX-500E from Mason Technology, Ireland, was  
80 used for all experiments and solution preparations.

### 81 2.2. Synthesis of colloidal GNPs

82 A 1 mM stock solution of chloroauric acid was made by dissolving hydrogen tetrachloroaurate  
83 in water. The 10 mM HEPES buffer stock solution was made by diluting 1 mM HEPES buffer,  
84 purchased from Sigma Aldrich (Ireland), with water. Different concentrations of monosodium  
85 phosphate and disodium phosphate solutions were prepared by dissolving in water, accordingly.

86 In the standard synthesis of GNPs, which will be referred to as 'Standard' in the following  
87 sections, 200  $\mu\text{L}$  of 1 mM chloroauric acid were mixed with 200  $\mu\text{L}$  of 10 mM HEPES buffer and 600  
88  $\mu\text{L}$  of water. After 10-15 minutes, the colour of the solution changed from pale yellow to colourless,  
89 then eventually changed to pink, indicating the formation of GNPs

90 In the synthesis of GNPs using phosphates, a similar procedure was followed, with the  
91 exception that 200  $\mu\text{L}$  of 1 mM chloroauric acid were mixed with 200  $\mu\text{L}$  of 10 mM HEPES buffer  
92 and 600  $\mu\text{L}$  of monosodium phosphate or disodium phosphate solution, of systematically varied  
93 concentrations.

94 For all GNP samples, the mass concentration of gold is 39.394 mg/L.

### 95 2.3. Characterisation of GNPs

96 The absorption spectrum of the GNPs in the ultraviolet-visible spectral region was measured  
97 using a Perkin Elmer Lambda 900 UV/VIS/NIR Spectrometer. The absorption spectrum was used to  
98 monitor the formation of GNPs, and to characterise and discriminate different samples.

99 The formation time of GNPs was recorded, defined as the amount of time from the start of the  
100 reaction to the time point at which the ratio of the light absorption of GNPs at 540 nm ( $A_{540}$ ) and the  
101 absorption at 450 nm ( $A_{450}$ ) was higher than 1 [32-34].

102 A Hitachi SU6600 FESEM instrument was used to record images of different kinds of GNPs  
103 synthesised with or without phosphates. Three representative formulations of GNPs were  
104 prepared, named as, Standard, 6mM of monosodium phosphate and 6mM of disodium phosphate.  
105 In the synthesis of GNPs using phosphates, 200  $\mu$ L of 1 mM chloroauric acid were mixed with 200  
106  $\mu$ L of 10 mM HEPES buffer and 600  $\mu$ L of 6mM of monosodium phosphate and 6mM of disodium  
107 phosphate solution were used respectively. After reaction for 1.5 hours, the samples were dropped  
108 onto silicon wafers and spun for 2.5 minutes to dry in the air. The samples on silicon substrates  
109 were then observed under the scanning electron microscope within 2 days. An accelerating voltage  
110 of 20 kV was used for all samples.

111 The hydrodynamic particle sizes and zeta potentials of different samples were also measured,  
112 using a Zetasizer Nano ZS Analyser from Malvern Instruments, Worcestershire, UK.

113 The pH values of the GNP synthesis systems with different concentrations of monosodium  
114 phosphates or disodium phosphates added were measured using Thermo Scientific™ Orion™ 3-  
115 Star Benchtop pH Meter.

### 116 2.4. Toxicity test of GNPs on fungi

117 The toxicity of the Standard GNP and GNPs synthesised using phosphates was tested. Three  
118 species of fungus, *Aspergillus niger*, *Mucor hiemalis* and *Penicillium chrysogenum* were used in the  
119 toxicity test. The fungi samples were prepared by inoculating each in a bottle of sterilised and  
120 deionised water and then examined as prepared, and the survival and growth of fungi was  
121 measured using the plate count method as described previously [35].

122 Briefly, for each species of fungus, a comparison group and a test group were prepared and  
123 incubated at the same time. In the comparison group, mixtures of 10 mM HEPES buffer and  
124 deionised water or different concentrations of monosodium or disodium phosphates at a ratio of 1:3  
125 were prepared. Then these mixtures were adjusted using sodium hydroxide and/or hydrochloride  
126 acid until the pH values were 7. Then the fungus sample was mixed with each mixture at a ratio of  
127 1:1 and each spread on the potato dextrose agar (PDA) plates. In the test group, the GNPs were  
128 synthesised using phosphates with the same concentrations as in the comparison group, and the  
129 pH values were adjusted to 7 with sodium hydroxide and hydrochloride acid, then mixed with  
130 fungus samples at a ratio of 1:1 and spread on the PDA plates. The GNP exposure dose for all  
131 samples is 19.697 mg/L gold. In total, for each kind for fungi, 8 pairs of comparison group and test  
132 group were prepared, which includes Standard GNP, 3 kinds of GNPs synthesised adding  
133 monosodium phosphate, and 4 kinds of GNPs synthesised adding disodium phosphate.

134 All chemicals used in the comparison and test groups were sterilised in advance, and  
135 triplicates were measured for all test plates. All plates were incubated at 28°C for 48 hours, and then  
136 the colony-forming units (CFUs) were counted. The CFU result of each test group was divided by  
137 the CFU result of corresponding comparison group, indicating relative survival rate. During the  
138 process of pH adjustment, for all samples, to minimise the change in volume, high concentrations of  
139 sodium hydroxide and hydrochloride acid, namely 1 M and 5 M NaOH stock solution and 1 M and  
140 5 M HCl stock solution, were used. For each 3 mL sample solution, less than 20  $\mu$ L base or acid was  
141 added. Samples with base/acid added was shaken for 1 minute to mix properly, then measured  
142 with pH meter. After pH value adjusted to 7, samples were sterilised and ready for mixing with  
143 fungi sample.

144

## 145 2.5. Statistical Analysis

146 A paired t-test with two-tailed P value and 95% confidence interval was employed to evaluate  
 147 the difference between the survival rates of the comparison group and the experimental group for  
 148 the evaluation of toxicity. All statistical analyses are carried out using the software GraphPad Prism  
 149 7.

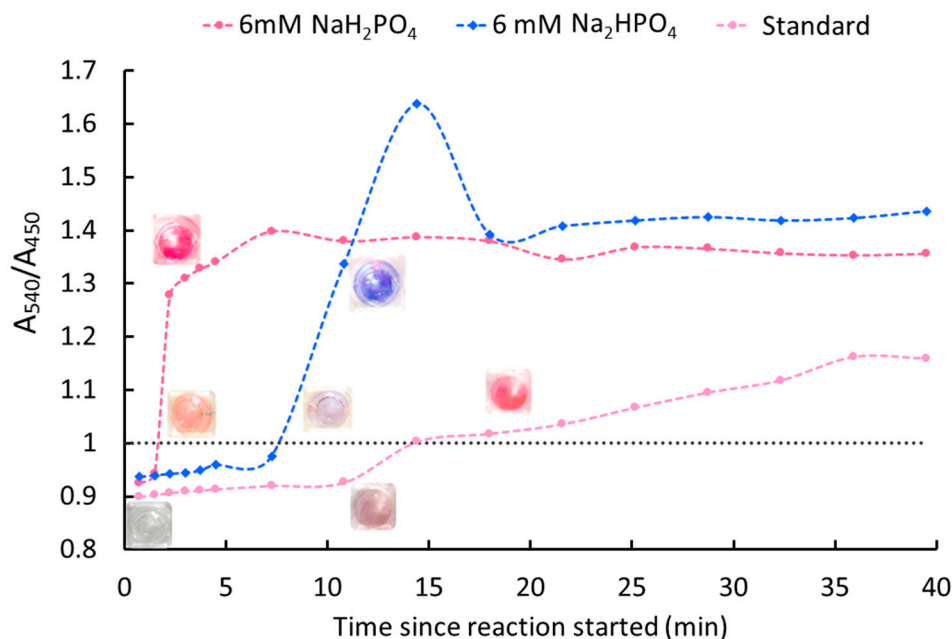
## 150 3. Results

## 151 3.1. GNP formation time

152 As the formation of GNPs progresses, the colour changes from colourless to  
 153 pink/purple/blue and the absorption spectrum of GNPs evolves, most significantly in terms of the  
 154 relative absorption at 540 nm and at 450 nm. Thus, the ratio between these two absorptions  
 155 ( $A_{540}/A_{450}$ ) has been selected to define the formation time of GNPs.

156 The ratio  $A_{540}/A_{450}$  changes as the formation of GNP progresses, along with (see **Figure 1**). A  
 157 dramatic increase, within 3 minutes or less, is observed for the synthesis using phosphate, during  
 158 which time the colour changes from colourless into pink/blue; for the standard synthesis  
 159 (Standard), the absorption ratio  $A_{540}/A_{450}$  increases much slowly as the colour changes slowly  
 160 from colourless to pale pink and eventually into pink.

161 Since the ratio changes rapidly from less than 1 into more than 1, 1 is defined as the critical  
 162 point of GNP formation. Once  $A_{540}/A_{450}$  is higher than 1, the formation of GNP is considered  
 163 complete, and the time from the start of the reaction to the time point when  $A_{540}/A_{450}$  equalled 1  
 164 was recorded accordingly as the GNP formation time.



165

166 **Figure 1.** The ratio of the light absorption of GNPs at 540 nm to that at 450 nm changes as a  
 167 function of reaction time during GNP formation. The colour changes of GNPs have also been  
 168 presented accordingly.

## 169 3.2. Characterisation of GNPs

170 The measured physicochemical characteristics of each kind of GNP are shown in **Table 1**.

171 For GNPs synthesised by adding monosodium phosphates, as the concentration of  
 172 monosodium phosphate increases, the GNP formation time shortens, and the absolute value of zeta  
 173 potential increases.

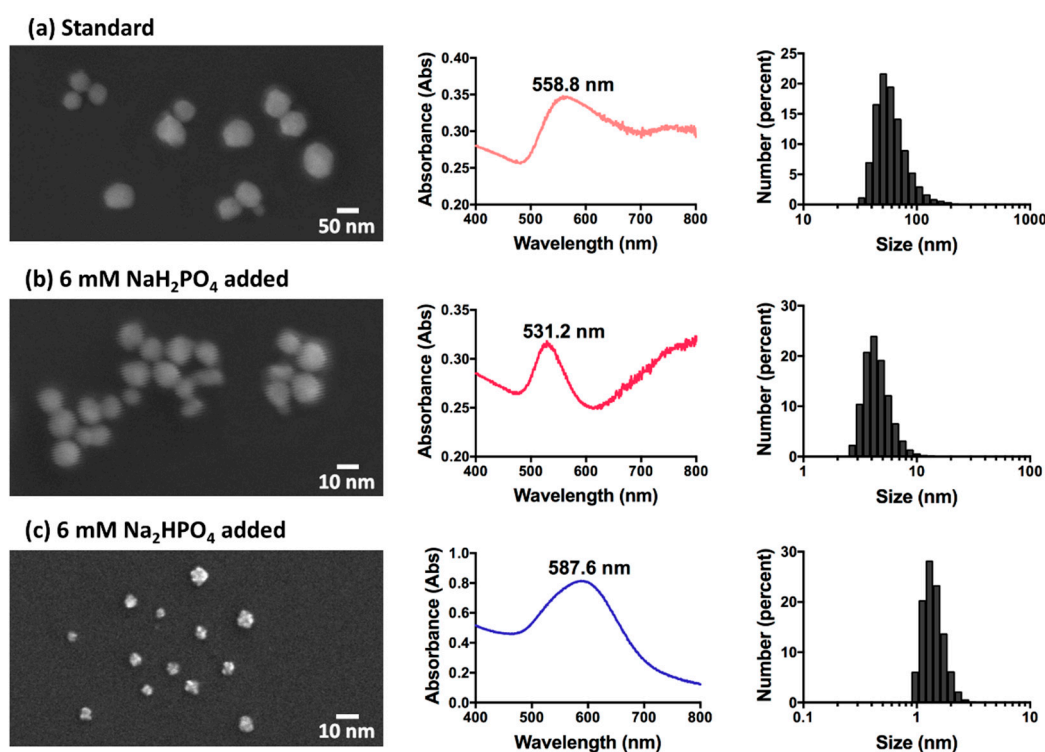
174 In contrast, for GNPs synthesised by adding disodium phosphates, both the formation time  
175 and absolute value of zeta potential decrease as the concentration of disodium phosphate increases.

176 While the average hydrodynamic size of Standard GNP is ~62 nm, the GNPs synthesised by  
177 adding monosodium phosphate reach the smallest size of ~4.6 nm in diameter when 6 mM  
178 monosodium phosphate are added, and higher or lower concentration of phosphate leads to larger  
179 particles. The diameters of GNPs synthesised adding disodium phosphates remain smaller than 53  
180 nm when the concentration of phosphate is lower than 100 mM, and particle sizes grow larger with  
181 the increase of disodium phosphate concentration after that.

182 **Table 1.** Physicochemical characteristics of the GNPs synthesised using different phosphates.

Sample <sup>1</sup>	Shape	Concentration of phosphate added (mM)	Formation time (min ± SD)	LSPR peak (nm)	Diameter (nm ± SD)	Zeta potential (mV ± SD)
Standard	Circular	0	15.00 ± 0.53	558.8	61.69 ± 22.35	-23.50 ± 0.21
NaH <sub>2</sub> PO <sub>4</sub> added	Circular	2	6.50 ± 0.25	565.0	82.33 ± 35.86	-26.43 ± 0.13
		6	1.50 ± 0.08	531.2	4.60 ± 1.32	-29.67 ± 0.13
		40	0.02 ± 0.01	532.2	634.54 ± 224.30	-36.87 ± 0.45
Na <sub>2</sub> HPO <sub>4</sub> added	Star-shaped/ Flower-shaped	1	12.50 ± 0.41	625.8	52.26 ± 14.94	-40.80 ± 0.24
		6	8.25 ± 0.27	587.6	1.42 ± 0.32	-34.97 ± 0.35
		50	2.83 ± 0.14	543.4	0.74 ± 0.25	-23.73 ± 0.60
		240	0.83 ± 0.01	664.0	391.05 ± 153.47	-22.13 ± 0.27

183 <sup>1</sup> Sample refers to the GNP synthesis methods. "Standard" refers to the GNPs synthesised using standard  
184 synthesis protocol. "NaH<sub>2</sub>PO<sub>4</sub> added" and "Na<sub>2</sub>HPO<sub>4</sub> added" refers to the GNPs synthesised adding different  
185 concentrations of monosodium and disodium phosphates accordingly.



186

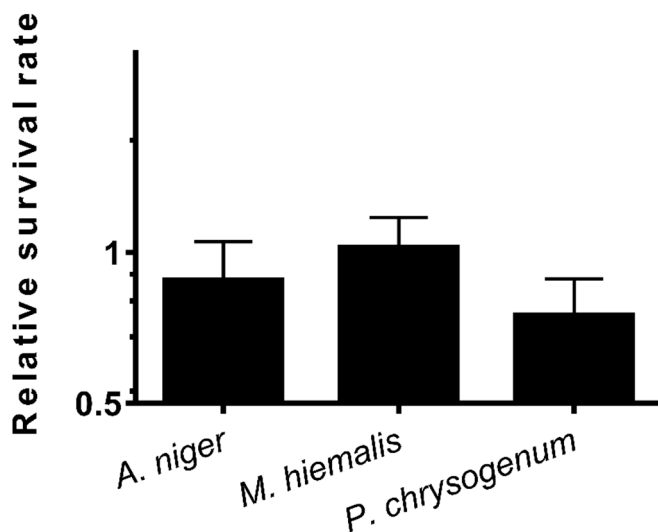
187 **Figure 2.** SEM images of GNPs with different sizes and shapes, and the corresponding UV-VIS  
188 spectra and size number distribution histogram (from left to right). (a) Standard GNPs synthesised  
189 with only chloroauric acid and HEPES buffer. (b) GNPs synthesised with chloroauric acid, HEPES  
190 buffer and 6 mM monosodium phosphate. (c) GNPs synthesised with chloroauric acid, HEPES  
191 buffer and 6 mM disodium phosphate.

192 The shape and size differences of the GNPs were analysed under SEM. The Standard and those  
 193 synthesised with monosodium phosphate are all circular-shaped, as shown in **Figure 2 a** and **b**.  
 194 However, even though they are both gold nanospheres, the diameter of the Standard GNPs is about  
 195 30-100 nm, while the diameter of those synthesised with 6 mM monosodium phosphate is much  
 196 smaller, ~2-10 nm. The GNPs synthesised by adding higher concentrations of monosodium  
 197 phosphate tend to aggregate into large clusters, which results in a UV-VIS peak at 800nm, and a  
 198 large scattering background to the UV-vis spectra.

199 In **Figure 2 c**, it can be inferred that the GNPs synthesised with 6 mM disodium phosphate are  
 200 star-shaped or flower-shaped, which explains the phenomenon that, although most GNPs with an  
 201 LSPR peak of more than 580 nm and a blue colour are aggregated or large sized, these appear to be  
 202 rather smaller, with diameters of only 1-3 nm.

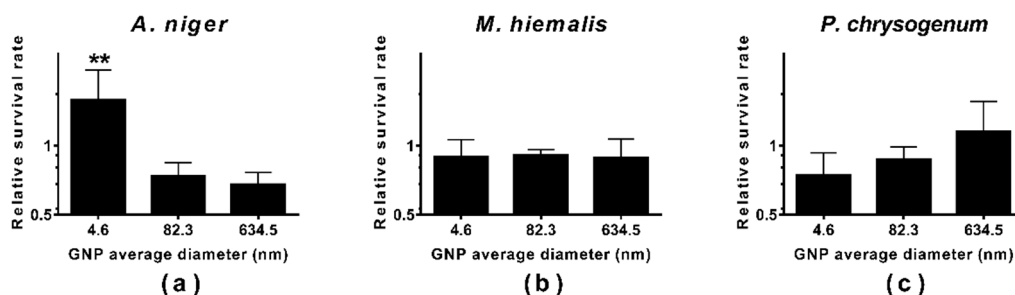
### 203 3.3. Toxicity test of GNPs with different sizes and shapes on fungi

204 After mixing pH adjusted HEPES and Standard GNP with *A. niger*, *M. hiemalis* and *P.*  
 205 *chrysogenum* and incubating for 48 hours, the fungal growth on each plate was compared by  
 206 calculating relative survival rates (**Figure 3**). It can be seen that *P. chrysogenum* shows the lowest  
 207 relative survival rate, followed by *A. niger*, and *M. hiemalis* has the highest relative survival rate at  
 208 ~1, which indicates that Standard GNP (19.697 mg/L gold) inhibits the growth of *P. chrysogenum*  
 209 and *A. niger*, while is not toxic to *M. hiemalis*.



210

211 **Figure 3.** Toxicity of Standard GNP to fungi. Comparisons between the relative survival rates of *A.*  
 212 *niger*, *M. hiemalis* and *P. chrysogenum* are shown.



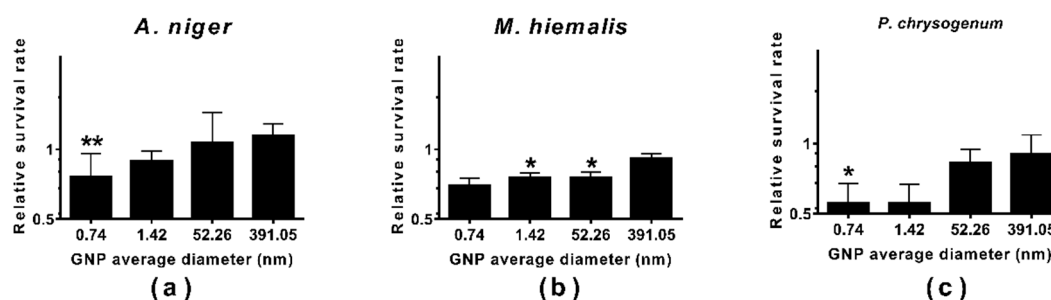
213

214 **Figure 4.** Toxicity of spherical GNPs synthesised with monosodium phosphates added to fungi.  
 215 Comparisons between the relative survival rates of (a) *A. niger*, (b) *M. hiemalis* and (c) *P. chrysogenum*  
 216 are shown. The T-test results between each pair of comparison group and test group are also shown.  
 217 (\*\* represents  $P < 0.005$ )

218 While the relative survival rates of *A. niger* mixed with 2 larger GNPs were less than 1, which  
 219 indicates that GNPs with those 2 sizes inhibited the growth of *A. niger*, the GNP sized ~4.6 nm  
 220 promoted the growth of *A. niger* with a relative survival rate of more than 1.5 (Figure 4 a).

221 In contrast, for *P. chrysogenum*, the smaller the GNP, the higher the toxicity. As shown in  
 222 Figure 4 c, the relative survival rate increased as the GNP average diameter got larger; the GNP  
 223 sized ~4.6 nm inhibited the growth, the GNP sized ~82 nm didn't have much influence the growth,  
 224 and the GNP sized ~635 nm promoted the growth of *P. chrysogenum*.

225 On the other hand, the GNPs synthesised by adding monosodium phosphates didn't have  
 226 much influence on the growth of *M. hiemalis*, since the relative survival rates of *M. hiemalis* mixed  
 227 with 3 sizes of GNP were all ~1 (Figure 4 b).



228

229 **Figure 5.** Toxicity of star-shaped GNPs synthesised adding disodium phosphates to fungi.  
 230 Comparisons between the survival rates of (a) *A. niger*, (b) *M. hiemalis* and (c) *P. chrysogenum* are  
 231 shown. The T-test results between each pair of comparison group and test group are also shown. (\*  
 232 represents  $P < 0.05$ , \*\* represents  $P < 0.005$ )

233 For all three kinds of fungi, it appears that the smaller the size of GNP synthesised using  
 234 disodium phosphates, the lower the relative survival rate (Figure 5), which indicates that smaller  
 235 GNPs have higher toxicity to these three kinds of fungi.

236 The small GNPs, with diameters less than 2 nm, inhibited the growth of *A. niger*, while GNPs  
 237 larger than ~50 nm promoted the growth (Figure 5 a).

238 On the other hand, GNPs of all 4 sizes used inhibited the growth of both *M. hiemalis* and *P.*  
 239 *chrysogenum*, as all relative survival rates were seen to be lower than 1 (Figure 5 b, c). While the  
 240 largest GNP decreased the growth of these two fungi only slightly, the relative survival rate of *P.*  
 241 *chrysogenum* dropped significantly upon expose to the smaller GNPs, although *M. hiemalis* reacted  
 242 less sensitively.

243 Paired t-tests with two-tailed P value and 95% confident interval were employed to compare  
 244 survival rates between the comparison group and experimental group for each concentration and  
 245 each fungi, and results are shown in Figure 3, 4, 5.

246 In general, after comparing the survival rates of comparison groups and experimental groups,  
 247 Standard GNP decreases the growth of *P. chrysogenum* most, followed by *A. niger*, while exposure  
 248 has little effect on *M. hiemalis*. The GNPs synthesised using monosodium phosphates didn't show  
 249 much size dependent trends in the effects on the relative survival rates of fungi: while larger GNP  
 250 inhibited the growth of *A. niger* strikingly, smaller GNPs decreased the relative survival rate of  
 251 *P. chrysogenum* most, and *M. hiemalis* was not much effected. In contrast, the GNPs synthesised  
 252 using disodium phosphates showed significant size trends, as smaller GNP were seen to exhibit  
 253 stronger toxicity to fungi, and the growth of *P. chrysogenum* was inhibited most significantly,  
 254 followed by *M. hiemalis*, and *A. niger* with minimum influence.

255

## 256 4. Discussion

### 257 4.1. Ensuring reproducibility of GNP mass concentrations

258 Various methods for the synthesis of GNP have been developed with limited knowledge of  
259 potential environmental toxicity. In our study, we assessed toxicity in fungi using GNP synthesised  
260 by 3 different methods: Standard GNP, GNPs synthesised adding monosodium phosphates, and  
261 GNPs synthesised using disodium phosphates. In order to accurately compare toxicities of GNP  
262 produced using three methods, we needed to ensure the reproducibility of mass concentration of  
263 GNP produced. All samples, whether with phosphates added or not, were synthesised by mixing  
264 200  $\mu\text{L}$  of 1 mM chloroauric acid and 200  $\mu\text{L}$  of 10 mM HEPES buffer for every 1 mL sample.

265 The HEPES reduced GNP synthesis method has been applied and studied for a decade, and it  
266 has been reported that the difference of the molar ratio of chloroauric acid and HEPES strongly  
267 affects the GNP synthesised [30]. In this study, a molar ratio of 1:10 between chloroauric acid and  
268 HEPES has been applied to all syntheses, which ensured the complete reduction of chloroauric acid  
269 into atomic gold. Thus, the mass concentration of gold for all GNP samples is the same, which  
270 allows their toxicities to be compared since the volumes of GNPs mixed with all fungi samples are  
271 the same, leading to same exposure dose as 19.697 mg/L for all samples,

272 While a formation time of ~15 minutes is needed for a typical synthesis protocol using HEPES,  
273 the addition of monosodium phosphate or disodium phosphate accelerates the formation process of  
274 the GNPs (see **Table 1**). This could be because the addition of phosphate brings more ions into the  
275 reaction system, which provides a more suitable formation environment and thus shortens the  
276 formation time.

277 The LSPR peaks of the GNPs synthesised using phosphates are also different to the Standard  
278 GNP (**Table 1**). As reported by Haiss et al., the size and concentration of GNPs within the size  
279 range of 5-100 nm can be directly determined from UV-VIS spectra according to corrected Mie  
280 theory[36]. While GNP with average hydrodynamic diameter ~62 nm and LSPR peak of 558.8 nm  
281 can be synthesised using a typical standard protocol, GNPs sized ~4-85 nm can be synthesised  
282 when adding 2-6 mM monosodium phosphate, and GNPs sized 0.7-55 nm can be synthesised when  
283 1-50 mM disodium phosphate is added (**Table 1**). For these GNP samples, the smaller the  
284 diameters, the lower the LSPR peak wavelengths according to corrected Mie theory[36].

### 285 4.2. Comparing toxicity of GNPs

286 Both Standard GNP and GNPs synthesised by adding monosodium phosphates are spherical  
287 in shape (**Figure 2**), but the size of particles range from as small as 3-10 nm, to aggregates as large as  
288 ~650 nm (**Table 1**). It appears that when the shapes of GNPs are the same, the sizes of the GNPs  
289 influence the relative survival rates of fungi differently.

#### 290 4.2.1. Toxicity of Standard GNPs

291 Standard GNPs are circular shaped particles with diameters range from 30 nm to 100 nm  
292 (**Figure 2 a**), and an average hydrodynamic diameter of ~62 nm (**Table 1**).

293 As shown by the results in **Figure 3**, the growth of *P. chrysogenum* was inhibited considerably  
294 after exposure to Standard GNP, compared to the group mixed with HEPES alone. Similarly, the  
295 growth of *A. niger* was inhibited by Standard GNP, while the survival rate of *M. hiemalis* only  
296 decreased a little (**Figure 3**).

297 The flourishing growth of the group mixed with HEPES and GNP could be caused by the extra  
298 nutrition provided by HEPES. However, compared to the comparison group, Standard GNP still  
299 showed a strong decrease of the survival rate, indicating that the Standard GNP is toxic to *P.*  
300 *chrysogenum*. On the other hand, the growth of *A. niger* was inhibited by Standard GNP in  
301 comparison, which indicates that Standard GNP is also toxic to *A. niger*, but to a lesser extent than  
302 to *P. chrysogenum*. Comparing to comparison group, Standard GNP didn't cause much influence on  
303 the growth of *M. hiemalis*, which indicates that Standard GNP has little toxicity to it.



#### 304 4.2.2. Toxicity of GNPs synthesized adding monosodium phosphates

305 The sizes of GNPs synthesised vary as the concentration of monosodium phosphates added is  
306 varied. The GNP synthesised by adding 6 mM monosodium phosphate exhibit the smallest average  
307 hydrodynamic diameter of ~4.6 nm (**Table 1**), with most particles sized between 2-10 nm (**Figure 2**).  
308 The GNPs synthesised by adding 2 mM monosodium phosphate are larger, with average  
309 hydrodynamic diameter of ~82 nm, and those produced by adding 40 mM monosodium phosphate  
310 form large aggregates with sizes ~635 nm (**Table 1**).

311 For *A. niger*, the growth was significantly increased upon the exposure to the smallest GNP,  
312 while the growth decreased slightly when exposed to the larger GNPs (**Figure 4 a**). The survival  
313 rates of *A. niger* mixed with GNPs sized ~82 nm and ~635 nm are only slightly lower than the  
314 comparison groups. And the growth increase of the one added with smallest GNP could be caused  
315 by the higher phosphate absorption. It has been reported that the phosphate is essential for the  
316 growth of mold fungi, including *Aspergillus*, *Penicillium* and *Rhizopus* [37]. For *A. niger*, the  
317 phosphates absorbed are converted into different phosphorus compounds, most of which are acid-  
318 hydrolysable compounds [38], and as much as 90% of these are accumulated in the mycelia [39].  
319 Since the size of this GNP is very small, the particles are absorbed easier by *A. niger*, along with the  
320 phosphate ions attached to the particles. So, the higher absorption of phosphates may lead to the  
321 enhanced growth. In general, it cannot be determined whether the GNPs synthesised adding  
322 monosodium phosphate have much influence on the growth of or toxicity to *A. niger*.

323 For *P. chrysogenum*, it can be seen that the relative survival rates are decreased significantly  
324 upon exposure to GNPs, and the one mixed with smallest GNP has the least growth (**Figure 4 c**). It  
325 can be inferred that the 4.6 nm GNP, which is circular, relatively the smallest and synthesised using  
326 6 mM monosodium phosphate, has strongest toxicity to *P. chrysogenum*.

327 For *M. hiemalis*, the growth was only slightly decreased by GNPs synthesised using  
328 monosodium phosphates (**Figure 4 b**). The reason is likely due to the presence of higher  
329 concentrations of phosphate which increases the cellular activities of *M. hiemalis* and causes it to  
330 grow more rapidly [39], which minimised the effects of GNPs.

331 In general, *P. chrysogenum* reacts most sensitively to the toxicity of circular-shaped GNPs, and  
332 the smaller the particle size, the stronger the toxicity, while these GNPs showed contrary size trends  
333 on *A. niger*, and have little effect on *M. hiemalis*.

#### 334 4.2.3. Toxicity of star/flower-shaped GNPs

335 The sizes of GNPs synthesised by adding disodium phosphates are smallest when  
336 concentrations of disodium phosphates added are between 6-50 mM, followed by those formed by  
337 adding 1 mM disodium phosphate. When the concentration is higher than 100 mM, the particle  
338 sizes become very large, with average hydrodynamic diameters larger than 280 nm (**Table 1**). The  
339 shape of GNPs is flower-like and/or star-like, as shown in **Figure 2 c**.

340 From **Figure 5 a**, it can be seen that the *A. niger* mixed with GNP sized ~0.74 nm have the  
341 largest decrease of relative survival rate. It can be inferred that the flower-shaped GNPs smaller  
342 than 10 nm have toxicity on *A. niger*. The increase in relative survival rates of *A. niger* could be  
343 because higher concentrations of phosphates promoted the growth.

344 For *M. hiemalis*, all relative survival rates were decreased (**Figure 5 b**), especially the ones  
345 mixed with the smallest GNP. It can be inferred that the flower/star-shaped GNPs have toxicity on  
346 *M. hiemalis* as well, with smaller GNPs eliciting higher toxicity.

347 For *P. chrysogenum* (**Figure 5 c**), the relative survival rates also decreased sufficiently, especially  
348 for 0.74 nm GNP, which is synthesised by adding 50 mM disodium phosphate. It can be inferred  
349 that the GNPs synthesised with disodium phosphate added are very toxic to *P. chrysogenum*.

350 In general, the star/flower-shaped GNPs are toxic to all three kinds of fungi, with highest  
351 toxicity to *P. chrysogenum*, followed by *M. hiemalis* and least toxicity to *A. niger*.

352

#### 353 4.4. Toxicity comparison between different shaped GNPs

354 Since the size of circular-shaped GNP synthesised adding 6 mM monosodium phosphate is  
355 similar to the sizes of star/flower-shaped GNPs synthesised adding 6-50 mM disodium phosphates,  
356 their effects on the growth of each kind of fungi are compared to see the shape effect of GNP's  
357 toxicity.

358 From **Figure 4 a** and **Figure 5 a**, it can be seen that the toxicity of star/flower shaped GNPs is  
359 clearly stronger than circular-shaped GNP on *A. niger*. While circular-shaped GNPs do not have  
360 much effect on the growth of *A. niger*, the star/flower-shaped GNPs decreased the relative survival  
361 rates significantly.

362 For *M. hiemalis*, the difference of the toxicities is small, since both circular-shaped and  
363 star/flower-shaped GNPs decreased the relative survival rates to similar extents (**Figure 4 b** and  
364 **Figure 5 b**).

365 When comparing results from **Figure 4 c** and **Figure 5 c**, it can be inferred that the toxicity of  
366 star/flower-shaped GNPs on *P. chrysogenum* is higher than circular-shaped GNPs, since the former  
367 decreased the survival rates to a larger extent.

#### 368 5. Conclusions

369 The role of shape and size of GNPs on their toxicities on 3 kinds of fungi, *A. niger*, *M. hiemalis*  
370 and *P. chrysogenum*, were investigated. Two kinds of GNP shape, circular and star/flower-like  
371 shaped, with different sizes were examined. The circular-shaped GNPs were synthesised using 2  
372 kinds of methods: the standard synthesis method, which creates Standard GNP with average  
373 hydrodynamic diameter of 62 nm; and the synthesis method adding different concentrations of  
374 monosodium phosphates, which creates GNPs sized between 4.6 nm to 85 nm, and large aggregates  
375 sized 635 nm. The star/flower-shaped GNPs were synthesised by adding different concentrations of  
376 disodium phosphates and were sized between 0.7 nm and 400 nm.

377 It has been found that, under the exposure dose of 19.7 mg/L gold, the Standard GNP has  
378 relatively highest toxicity to *P. chrysogenum*, followed by *A. niger*, and has least toxicity to *M.*  
379 *hiemalis*. For circular-shaped GNPs synthesised using monosodium phosphates, *P. chrysogenum*  
380 reacts most sensitively to their toxicity, and smaller GNPs show stronger toxicity; while the size  
381 trends are contrary for *A. niger*, and these GNPs have little toxicity to *M. hiemalis*.

382 It has also been found that, under the same mass concentration exposure dose, star/flower-  
383 shaped GNPs have very strong toxicity to *P. chrysogenum*, less toxicity to *M. hiemalis*, and least  
384 toxicity to *A. niger*. Similarly, for all three kinds of fungi, smaller sized star/flower-shaped GNP  
385 exhibit stronger toxicity.

386 The size effect of GNP's toxicity could be caused by the easier absorption of smaller particles.  
387 When comparing similar sized GNPs with same mass concentration, it was shown that for *P.*  
388 *chrysogenum* and *A. niger*, the star/flower-shaped GNPs have higher toxicity than circular-shaped  
389 GNPs, while the shape of GNPs do not have much effect on the toxicity to *M. hiemalis*.

390 **Supplementary Materials:** The following are available online at [www.mdpi.com/link](http://www.mdpi.com/link), Figure S1: Size and zeta  
391 potential of GNPs synthesised using phosphates, Figure S2: Toxicity of GNPs synthesised with monosodium  
392 phosphate on fungi, Table S1: The size and zeta potential of GNPs synthesised using monosodium phosphate  
393 and disodium phosphate.

394 **Acknowledgments:** K.L. thanks Fiosraigh Scholarship Programme from Dublin Institute Technology. F.T.  
395 acknowledges Enterprise Ireland CF-2015-0269-Y.

396 **Author Contributions:** K.L. and F.T. conceived and designed the experiments; K.L. performed the  
397 experiments; K.L. and Z.H. analysed the data; K.L. and F.T. contributed reagents/materials/analysis tools; K.L.,  
398 Z.H., H.J.B., J.C. and F.T. wrote the paper.

399 **Conflicts of Interest:** The authors declare no conflict of interest.

400

401 **References**

- 402 1. Toshima, N. Nanoscale materials. *M. Liz-Marzan L., Kamat PV,(Eds.), Kluwer Academic Pub., London*  
403 **2003**, 79-96.
- 404 2. Rotello, V.M. *Nanoparticles: Building blocks for nanotechnology*. Springer Science & Business Media:  
405 2004.
- 406 3. Rogach, A.; Talapin, D.; Weller, H.; Caruso, F. Colloids and colloid assemblies. *Edited by Frank Caruso,*  
407 *Wiley-VCH Verlag GmbH & Co. KGaA, Weinheim 2004*.
- 408 4. Schmid, G. *Nanoparticles: From theory to application*. John Wiley & Sons: 2011.
- 409 5. Sreeprasad, T.S.; Pradeep, T. Noble metal nanoparticles. In *Springer handbook of nanomaterials*,  
410 Springer: 2013; pp 303-388.
- 411 6. Willets, K.A.; Van Duyne, R.P. Localized surface plasmon resonance spectroscopy and sensing. *Annu.*  
412 *Rev. Phys. Chem.* **2007**, *58*, 267-297.
- 413 7. Petryayeva, E.; Krull, U.J. Localized surface plasmon resonance: Nanostructures, bioassays and  
414 biosensing—a review. *Analytica chimica acta* **2011**, *706*, 8-24.
- 415 8. Lu, X.; Rycenga, M.; Skrabalak, S.E.; Wiley, B.; Xia, Y. Chemical synthesis of novel plasmonic  
416 nanoparticles. *Annual review of physical chemistry* **2009**, *60*, 167-192.
- 417 9. Morones, J.R.; Elechiguerra, J.L.; Camacho, A.; Holt, K.; Kouri, J.B.; Ramírez, J.T.; Yacaman, M.J. The  
418 bactericidal effect of silver nanoparticles. *Nanotechnology* **2005**, *16*, 2346.
- 419 10. Jain, P.; Pradeep, T. Potential of silver nanoparticle-coated polyurethane foam as an antibacterial  
420 water filter. *Biotechnology and bioengineering* **2005**, *90*, 59-63.
- 421 11. Ahamed, M.; AlSalhi, M.S.; Siddiqui, M. Silver nanoparticle applications and human health. *Clinica*  
422 *chimica acta* **2010**, *411*, 1841-1848.
- 423 12. Wang, S.; Lawson, R.; Ray, P.C.; Yu, H. Toxic effects of gold nanoparticles on salmonella  
424 typhimurium bacteria. *Toxicology and industrial health* **2011**, *27*, 547-554.
- 425 13. Shah, V.; Belozeroval, I. Influence of metal nanoparticles on the soil microbial community and  
426 germination of lettuce seeds. *Water, Air, and Soil Pollution* **2009**, *197*, 143-148.
- 427 14. Zhao, Y.; Tian, Y.; Cui, Y.; Liu, W.; Ma, W.; Jiang, X. Small molecule-capped gold nanoparticles as  
428 potent antibacterial agents that target gram-negative bacteria. *Journal of the American Chemical Society*  
429 **2010**, *132*, 12349-12356.
- 430 15. Tian, F.; Clift, M.J.; Casey, A.; del Pino, P.; Pelaz, B.; Conde, J.; Byrne, H.J.; Rothen-Rutishauser, B.;  
431 Estrada, G.; de la Fuente, J.M. Investigating the role of shape on the biological impact of gold  
432 nanoparticles in vitro. *Nanomedicine* **2015**, *10*, 2643-2657.
- 433 16. Chithrani, B.D.; Ghazani, A.A.; Chan, W.C. Determining the size and shape dependence of gold  
434 nanoparticle uptake into mammalian cells. *Nano lett* **2006**, *6*, 662-668.
- 435 17. Alkilany, A.M.; Murphy, C.J. Toxicity and cellular uptake of gold nanoparticles: What we have  
436 learned so far? *Journal of nanoparticle research* **2010**, *12*, 2313-2333.
- 437 18. Wang, S.; Lu, W.; Tovmachenko, O.; Rai, U.S.; Yu, H.; Ray, P.C. Challenge in understanding size and  
438 shape dependent toxicity of gold nanomaterials in human skin keratinocytes. *Chemical physics letters*  
439 **2008**, *463*, 145-149.
- 440 19. Nowack, B.; Bucheli, T.D. Occurrence, behavior and effects of nanoparticles in the environment.  
441 *Environmental pollution* **2007**, *150*, 5-22.
- 442 20. Dunphy Guzman, K.A.; Taylor, M.R.; Banfield, J.F. Environmental risks of nanotechnology: National  
443 nanotechnology initiative funding, 2000–2004. ACS Publications: 2006.

- 444 21. Maynard, A.D. A research strategy for addressing risk. *Nanotechnology, Woodrow Wilson International*  
445 *Center for Scholars* **2006**.
- 446 22. Oberdörster, G.; Oberdörster, E.; Oberdörster, J. Nanotoxicology: An emerging discipline evolving  
447 from studies of ultrafine particles. *Environmental health perspectives* **2005**, *113*, 823.
- 448 23. Navarro, E.; Baun, A.; Behra, R.; Hartmann, N.B.; Filser, J.; Miao, A.-J.; Quigg, A.; Santschi, P.H.; Sigg,  
449 L. Environmental behavior and ecotoxicity of engineered nanoparticles to algae, plants, and fungi.  
450 *Ecotoxicology* **2008**, *17*, 372-386.
- 451 24. Colvin, V.L. The potential environmental impact of engineered nanomaterials. *Nature biotechnology*  
452 **2003**, *21*, 1166-1170.
- 453 25. Cheetham, N.W. *Introducing biological energetics: How energy and information control the living world*.  
454 Oxford University Press: 2010.
- 455 26. Moore, B.; Duncan, J.; Burgess, J. Fungal bioaccumulation of copper, nickel, gold and platinum.  
456 *Minerals Engineering* **2008**, *21*, 55-60.
- 457 27. Samson, R.A.; Houbraken, J.; Summerbell, R.C.; Flannigan, B.; Miller, J.D. Common and important  
458 species of fungi and actinomycetes in indoor environments.'. *Microorganisms in home and indoor work*  
459 *environments: diversity, health impacts, investigation and control* **2002**, 285-473.
- 460 28. Saleh, Y.; Mayo, M.; Ahearn, D. Resistance of some common fungi to gamma irradiation. *Applied and*  
461 *environmental microbiology* **1988**, *54*, 2134-2135.
- 462 29. Young, J.C.; Fulcher, R. Mycotoxins in grains: Causes, consequences, and cures. *Cereal foods world*  
463 **1984**.
- 464 30. Chen, R.; Wu, J.; Li, H.; Cheng, G.; Lu, Z.; Che, C.-M. Fabrication of gold nanoparticles with different  
465 morphologies in hepes buffer. *Rare Metals* **2010**, *29*, 180-186.
- 466 31. Habib, A.; Tabata, M.; Wu, Y.G. Formation of gold nanoparticles by good's buffers. *Bulletin of the*  
467 *Chemical Society of Japan* **2005**, *78*, 262-269.
- 468 32. Sojinrin, T.; Conde, J.; Liu, K.; Curtin, J.; Byrne, H.J.; Cui, D.; Tian, F. Plasmonic gold nanoparticles for  
469 detection of fungi and human cutaneous fungal infections. *Analytical and Bioanalytical Chemistry* **2017**,  
470 1-12.
- 471 33. Wei, H.; Li, B.; Li, J.; Wang, E.; Dong, S. Simple and sensitive aptamer-based colorimetric sensing of  
472 protein using unmodified gold nanoparticle probes. *Chemical Communications* **2007**, 3735-3737.
- 473 34. Kim, Y.S.; Kim, J.H.; Kim, I.A.; Lee, S.J.; Jurng, J.; Gu, M.B. A novel colorimetric aptasensor using gold  
474 nanoparticle for a highly sensitive and specific detection of oxytetracycline. *Biosensors and*  
475 *Bioelectronics* **2010**, *26*, 1644-1649.
- 476 35. Goldman, E.; Green, L.H. *Practical handbook of microbiology*. CRC Press: 2015.
- 477 36. Haiss, W.; Thanh, N.T.; Aveyard, J.; Fernig, D.G. Determination of size and concentration of gold  
478 nanoparticles from uv- vis spectra. *Analytical chemistry* **2007**, *79*, 4215-4221.
- 479 37. Foster, J.W. The heavy metal nutrition of fungi. *The Botanical Review* **1939**, *5*, 207-239.
- 480 38. Mann, T. Studies on the metabolism of mould fungi: 2. Isolation of pyrophosphate and  
481 metaphosphate from aspergillus niger. *Biochemical Journal* **1944**, *38*, 345.
- 482 39. Mann, T. Studies on the metabolism of mould fungi: 1. Phosphorus metabolism in moulds. *Biochemical*  
483 *Journal* **1944**, *38*, 339.